

ORTHO-TO-PARA ABUNDANCE RATIO (OPR) OF AMMONIA IN 15 COMETS: OPRs OF AMMONIA VERSUS $^{14}\text{N}/^{15}\text{N}$ RATIOS IN CN^{*,†}

YOSHIHARU SHINNAKA¹, HIDEYO KAWAKITA¹, HITOMI KOBAYASHI¹, EMMANUËL JEHIN^{2,3}, JEAN MANFROID^{2,3}, DAMIEN HUTSEMÉKERS^{2,3}, AND CLAUDE ARPIGNY²

¹ Kyoto Sangyo University, Department of Physics, Faculty of Science, Motoyama, Kamigamo, Kita-ku, Kyoto 603-8555, Japan

² Institut d’Astrophysique et de Géophysique Liège Université, Université de Liège, B-4000 Liège, Belgium

³ FRS-FNRS, Université de Liège, B-4000 Liège, Belgium

Received 2010 October 12; accepted 2011 January 2; published 2011 February 11

ABSTRACT

The ortho-to-para abundance ratio (OPR) of cometary molecules is considered to be one of the primordial characteristics of cometary ices. We present OPRs of ammonia (NH_3) in 15 comets based on optical high-dispersion spectroscopic observations of NH_2 , which is a photodissociation product of ammonia in the gaseous coma. The observations were mainly carried out with the VLT/UVES. The OPR of ammonia is estimated from the OPR of NH_2 based on the observations of the NH_2 (0, 9, 0) vibronic band. The absorption lines by the telluric atmosphere are corrected and the cometary C_2 emission lines blended with NH_2 lines are removed in our analysis. The ammonia OPRs show a cluster between 1.1 and 1.2 (this corresponds to a nuclear spin temperature of ~ 30 K) for all comets in our sample except for 73P/Schwassmann-Wachmann 3 (73P/SW3). Comet 73P/SW3 (both B- and C-fragments) shows the OPR of ammonia consistent with nuclear spin statistical weight ratio (1.0) that indicates a high-temperature limit as nuclear spin temperature. We compared the ammonia OPRs with other properties ($^{14}\text{N}/^{15}\text{N}$ ratios in CN, D/H ratios of water, and mixing ratios of volatiles). Comet 73P/SW3 is clearly different from the other comets in the plot of ammonia OPRs versus $^{14}\text{N}/^{15}\text{N}$ ratios in CN. The ammonia OPRs of 1.0 and lower ^{15}N -fractionation of CN in comet 73P/SW3 imply that icy materials in this comet formed under warmer conditions than other comets. Comets may be classified into two groups in the plot of ammonia OPRs against $^{14}\text{N}/^{15}\text{N}$ ratios in CN.

Key words: comets: general – ISM: clouds – ISM: molecules – protoplanetary disks

Online-only material: color figures

1. INTRODUCTION

Our solar system was formed from interstellar matter 4.6 Gyr ago. After the gravitational collapse of a molecular cloud core, the solar nebula (protoplanetary disk of the Sun) was formed. The planetesimals (of \sim km size), the building blocks of the planets, were accreted as rocky small bodies in the inner region of the solar nebula (asteroids) while planetesimals were mostly made of ice (but with dust grains) in the outer region. Remnants of those icy planetesimals are currently observed as comets.

Comets are defined as solar system small bodies that exhibit activities of outgassing and/or of mass loss (ejection of dust grains). The chemical composition of the gaseous “coma” (expanding atmosphere formed by sublimating ices from the nucleus) provides precious information to link the interstellar matter and the formation of our solar system. Similarity in chemistry between interstellar and cometary ices indicates that the comets incorporated the interstellar ices without any significant (or with very small) chemical alteration. However, the physical conditions of the pre-solar molecular cloud and their evolution are unclear so far.

Like the chemical composition of the cometary ice (usually we refer to the relative abundances of molecular species with respect to water, which is the most abundant molecule in cometary ice), isotopic ratios and abundance ratios of nuclear

spin isomers for some molecular species also give information about the formation conditions of the cometary molecules. In this paper, we concentrate on the abundance ratios between nuclear spin isomers of NH_3 in comets (ortho and para species for $I = 3/2$ and $I = 1/2$ where I denotes the total nuclear spin of identical H atoms).

Ortho-to-para abundance ratios (OPRs) of ammonia (NH_3) in comets were first measured in 2001. The OPR of water was determined from near-infrared spectroscopic observations in 1986 of comet 1P/Halley (Mumma et al. 1987) for the first time; the determination of OPR for NH_3 came later due to the difficulty of observing cometary NH_3 from ground-based observatories (until 1990s, firm detections of NH_3 lines in the radio range were reported in the case of two bright comets only, comet Hyakutake and comet Hale-Bopp). Although NH_3 lines were also detected by the near-infrared high-dispersion spectroscopic observations in this decade, the signal-to-noise ratios (S/Ns) of the measurements were not enough to determine the meaningful OPR of NH_3 in comets (Dello Russo et al. 2006). On the other hand, Kawakita et al. (2001) developed a new method for estimating the OPR of NH_3 from the high-dispersion optical spectrum of NH_2 . Thereafter, our group has reported the OPRs of NH_3 in several comets (Kawakita et al. 2001, 2002, 2004, 2006, 2007; Jehin et al. 2008, 2009a; Shinnaka et al. 2010). However, the number of comets sampled was still small.

The statistical weight ratio for nuclear spin species is unity for NH_3 in thermal equilibrium at the high-temperature limit, but the OPR of cometary NH_3 shows a cluster between 1.1 and 1.2. The real meaning of the OPR of NH_3 (as well as of water, methane, and other molecules) is still in debate (e.g.,

* Based on observations made with ESO Telescope at the La Silla Paranal Observatory under programs ID 268.C-5570, 270.C-5043, 073.C-0525, 274.C-5015, 075.C-0355(A), 080.C-0615, and 280.C-5053.

† Based on data collected at the Subaru Telescope, which is operated by the National Astronomical Observatory of Japan.

Table 1
Observational Data

Comet	Telescope/Instrument	Number of Observations	Heliocentric Distance (AU)	Geocentric Distance (AU)
C/1995 O1 (Hale-Bopp) ^a	D	1	0.92	1.33
C/1999 S4 (LINEAR) ^b	B	1	0.86	0.82
C/2001 A2 (LINEAR) ^c	B	1	1.39	0.46
153P/Ikeya-Zhang ^d	C	1	0.89	0.43
C/2000 WM ₁ (LINEAR) ^e	A	8	1.08–1.34	1.24
C/2002 V1 (NEAT) ^f	A	5	1.01–1.22	0.83–1.63
C/2002 X5 (Kudo-Fujikawa) ^f	A	6	0.70–1.07	0.86–0.99
C/2002 Y1 (Juels-Holvorcem) ^f	A	4	1.14–1.16	1.55–1.56
88P/Howell ^g	A	11	0.89–1.44	1.62–1.68
C/2001 Q4 (NEAT) ^h	A	10	0.97–0.98	0.32–0.32
C/2002 T7 (LINEAR) ^f	A	3	0.68–0.94	0.41–0.61
C/2003 K4 (LINEAR) ^f	A	1	1.20	1.51
9P/Tempel 1 ⁱ	A	10	1.51	0.89–0.94
73P-B/Schwassmann-Wachmann 3 ^j	A	1	0.94	0.25
73P-C/Schwassmann-Wachmann 3 ^j	A	1	0.95	0.15
8P/Tuttle ^k	A	3	1.03–1.04	0.36–0.62

Notes. A: VLT/UVES, B: Subaru/HDS, C: TNG/SARG, D: Xinglong 2.16 m Telescope/CES.

References. ^a Kawakita et al. 2004; ^b Kawakita et al. 2001; ^c Kawakita et al. 2002; ^d Capria et al. 2002; ^e Arpigny et al. 2003; ^f Manfroid et al. 2009; ^g Hutsemékers et al. 2005; ^h Manfroid et al. 2005; ⁱ Jehin et al. 2006; ^j Jehin et al. 2008; ^k Jehin et al. 2009b.

Bockelée-Morvan et al. 2009; Bonev et al. 2007, 2009; Crovisier 2006, 2007; Crovisier et al. 2008; Cacciani et al. 2009; Dello Russo et al. 2005; Jehin et al. 2008, 2009a, 2009b; Kawakita et al. 2002, 2004, 2005, 2006, 2007; Kawakita & Kobayashi 2009; Pardanaud et al. 2007; Woodward et al. 2007). One possible interpretation for the observed OPRs is “a nuclear spin temperature” (Mumma et al. 1987). The nuclear spin temperature (T_{spin}) and rotational excitation temperature (T_{rot}) can differ. A T_{spin} indicates the relation of populations between spin ladders while T_{rot} indicates the populations within the ladders.

Most measurements of NH_3 OPR indicate ~ 30 K as the nuclear spin temperature. Surprisingly, nuclear spin temperatures also cluster around 30 K in the case of water. This temperature, 30 K, seems to be a critical value for the formation of cometary molecules.

In this paper, we present a larger sample, with the OPRs of NH_3 measured in 15 comets of different types (including the reanalysis of those reported previously). We corrected the spectra for the influence of telluric transmittance (i.e., telluric absorption lines overlapped with the NH_2 lines) and removed the contamination of NH_2 lines by the C_2 Swan bands (such a correction was not considered in previous works). We discuss the real meaning of OPR based on the relationship between the OPRs and other properties.

2. THE DATA MATERIALS

In order to determine the OPR of cometary NH_3 , we observe NH_2 lines in the optical region and determine OPRs of NH_2 . The NH_2 radical is formed in the coma through the photodissociation of NH_3 by the solar UV radiation. Since the NH_2 radical has strong rovibronic transitions in the optical region (the $\tilde{A}-\tilde{X}$ system) caused by the solar fluorescence excitation mechanism, it is easy to obtain high S/N spectra of NH_2 in the coma. Here, we assume that NH_3 is the only parent of NH_2 in the coma (Kawakita & Watanabe 1998). As another possible parent of NH_2 , formamide (NH_2CHO) was discovered in comet Hale-Bopp but with an abundance of only 1%–2% relative to the NH_3 abundance (Bockelée-Morvan et al. 2000; Bird et al. 1997).

Hydrazine (N_2H_4) and methylamine (CH_3NH_2) may be other potential parents. However, we do not consider these potential parents here because these species have never been detected in cometary comae (Feldman et al. 2004). We can then assume that its contribution to the NH_2 production is negligible. In this case, the OPR value of NH_2 is related to that of NH_3 via the nuclear spin selection rules that are applied to the photodissociation reaction (Uy et al. 1997; Quack 1977). Thus, we can determine OPRs of NH_3 in comets from the observations of NH_2 .

The NH_2 (0,9,0)⁴ band has been used to determine the OPR of NH_2 in comets since this band is the strongest in the optical region for comets around 1 AU from the Sun and since it is not significantly affected by telluric absorption lines. Even though the NH_2 (0,9,0) band partially overlaps with the C_2 Swan sequence ($\Delta v = -2$), we can correct the contaminated NH_2 lines by using the fluorescence model of C_2 as demonstrated by Shinnaka et al. (2010). Details of the fluorescence excitation model of NH_2 are described in Section 3.

High-dispersion spectroscopic observations in the optical region were performed with different telescopes and instruments as follows:

1. the Ultraviolet and Visual Echelle Spectrograph (UVES; Dekker et al. 2000) mounted on the UT2 of the Very Large Telescope (VLT) at ESO Paranal, Chile,
2. the High Dispersion Spectrograph (HDS; Noguchi et al. 1998) mounted on the Subaru Telescope atop of Mauna Kea, Hawaii,
3. the cross-dispersed echelle spectrograph SARG (Gratton et al. 2001) mounted on the 3.5 m Telescopio Nazionale Galileo (TNG) at La Palma, Canary Islands, and
4. the Coudé Echelle Spectrograph (CES; Zhao & Li 2001) mounted on the Xinglong 2.16 m Telescope at Beijing Astronomical Observatory.

The details of the various observing runs of the 15 comets discussed here are summarized in Table 1.

⁴ The linear notation is employed for the \tilde{A} state here.

3. ANALYSIS AND MODELS

3.1. Fluorescence Excitation Model of NH_2

We used the fluorescence excitation model of NH_2 in the optical (Kawakita et al. 2000, 2001, 2004, 2006) to derive OPRs of NH_2 in the comets from their spectra of the NH_2 (0,9,0) band. In the model, we take into account the following.

1. the rovibronic transitions between $\tilde{\text{A}}(0, v_2', 0)$ and $\tilde{\text{X}}(0, 0, 0)$, $v_2' = 1-18$,
2. the rovibrational transitions of $\tilde{\text{X}}(0, v_2', 0)-\tilde{\text{X}}(0, 0, 0)$, $v_2' = 8-13$,
3. the rovibrational transition of $\tilde{\text{X}}(1, 0, 0)-\tilde{\text{X}}(0, 0, 0)$ and $\tilde{\text{X}}(0, 0, 1)-\tilde{\text{X}}(0, 0, 0)$,
4. the pure rotational transitions in $\tilde{\text{X}}(0, 0, 0)$, and
5. the fine structure of the energy levels (i.e., both F_1 and F_2 levels).

The fluorescence equilibrium is assumed for NH_2 . More detailed information about the fluorescence excitation model of NH_2 is described in the references listed above. Regarding the vibronic and vibrational transition moments of NH_2 , these were recently recalculated by Jensen et al. (2003) and updated in our model. The OPR of NH_2 is a free parameter in the model and is determined from a χ^2 fitting between the observed and modeled spectra.

3.2. Fluorescence Excitation Model of C_2

C_2 is one of the radicals that usually show prominent lines in the optical spectra of comets. The C_2 radical is a homonuclear diatomic molecule, and it is considered to be a daughter species (a photodissociation product) of more complex molecules (e.g., C_2H_2 , etc.). There are some strong emission bands around 4000–6000 Å (a.k.a. the Swan band sequences corresponding to the $d^3\Pi_g-a^3\Pi_u$ electric transition). The C_2 Swan sequence ($\Delta v = -2$) is recognized in the NH_2 (0,9,0) band region (~ 6000 Å). The contamination of NH_2 lines by C_2 lines should be removed to determine the OPR of NH_2 more accurately even if the C_2 lines are much weaker than the NH_2 lines.

We used the fluorescence excitation model of C_2 to remove the contamination of the NH_2 lines by the C_2 lines in the observed spectra. In this model, the Swan band sequences of $d^3\Pi_g-a^3\Pi_u$ are taken into account. For simplicity, we assume (1) the Boltzmann distribution at a given temperature (T_{rot}) in the lower state ($a^3\Pi_u$), and (2) the statistical equilibrium for the fluorescence excitation from the lower to the upper state ($d^3\Pi_g$). T_{rot} is determined by fitting the modeled spectra with the observations. The fluorescence excitation model of C_2 is also explained in Shinnaka et al. (2010).

3.3. Analysis

Data reduction was performed by the pipeline software customized for the instrument (in the case of UVES) and/or by the IRAF software package distributed from the NOAO⁵. The details for the reduction and calibration of the data obtained with VLT/UVES were described in Arpigny et al. (2003) and Jehin et al. (2004). The details for the reductions and calibrations of the data obtained with Subaru/HDS, TNG/SARG, and Xinglong 2.16 m Telescope/CES were described in Kawakita et al.

(2004). After the spectra are calibrated, we have to subtract the continuum component (the sunlight reflected by cometary dust grains) from the calibrated spectra. Since the continuum component is convolved with the telluric absorption lines of the atmosphere, we used the high-dispersion solar spectrum without telluric absorption lines (Kurucz 2005) and the synthesized telluric transmittance spectrum calculated by the LBLRTM code (Clough & Iacono 1995). We fitted the modeled transmittance with the observed spectra in the wavelength region where the continuum component is almost free from cometary lines. The fully resolved transmittance spectrum was convolved with a Gaussian function as the instrumental profile. The modeled continuum (the solar spectrum convolved with both the telluric transmittance and a reflectivity of dust grains) was fitted with the observations and then was subtracted from the observed spectrum.

We measured the emission flux of the NH_2 lines after removing all contamination by the C_2 lines based on the synthesized spectrum of the C_2 radical (Shinnaka et al. 2010) as described in the previous section. Then, we corrected the NH_2 flux for the telluric transmittance at the wavelength where each NH_2 line was observed. Note that the NH_2 (0,9,0) band is not severely affected by the telluric features. Figure 1 shows an example of both observed and modeled (best-fit) spectra of NH_2 in the case of C/2001 Q4 (NEAT). Finally, the OPR of ammonia could be estimated from the OPR of NH_2 determined from the comparison between observed and modeled spectra. Details of the analysis are described elsewhere (Shinnaka et al. 2010; Kawakita et al. 2001, 2004, 2006; Kawakita & Watanabe 2002).

The OPRs of both NH_2 and NH_3 determined from the observations are listed in Table 2. The weighted mean value and estimated errors of OPRs of NH_3 for each comet are given in Table 3.

4. RESULTS

4.1. Comet C/1995 O1 (Hale-Bopp)

The OPR of NH_3 in comet C/Hale-Bopp had already been reported in our previous study (Kawakita et al. 2004). The previous OPR of NH_3 was 1.21 ± 0.15 while the revised value is 1.17 ± 0.13 in this work. The small difference was caused by improvement in method for the data analysis. In the case of C/Hale-Bopp, the dust-to-gas ratio is very high, and the accuracy of the continuum subtraction is especially important for the measurements of the emission lines. In our analysis, the continuum component is modeled by convolving the solar spectrum with the synthesized telluric transmittance curve adjusted to the observational conditions. The T_{spin} is derived to be 28^{+12}_{-4} K for NH_3 (consistent with $T_{\text{spin}} = 28 \pm 2$ K derived from water lines in the same comet; Crovisier et al. 1997).

4.2. Comet C/1999 S4 (LINEAR)

Comet C/1999 S4 (LINEAR) broke into many fragments and disappeared before its perihelion passage during the 2000 apparition (Weaver et al. 2001). This comet was depleted in highly volatile species, and it might have formed in a warm region of the solar nebula, probably near Jupiter's orbit (Mumma et al. 2001a). Kawakita et al. (2001, 2004) had reported the OPR of NH_3 in this comet as 1.19 ± 0.06 while the revised value in this work is $\text{OPR} = 1.16 \pm 0.05$ indicating a $T_{\text{spin}} = 28^{+3}_{-2}$ K. This revised T_{spin} is consistent with the lower limit of

⁵ IRAF is distributed by the National Optical Astronomy Observatories, which are operated by the Association of Universities for Research in Astronomy, Inc., under cooperative agreement with the National Science Foundation.

Table 2
Ortho-to-Para Abundance Ratios of NH_2 and NH_3 of All Observations

Comet	Observational UT Data	Heliocentric Distance (AU)	NH_2 OPR	NH_3 OPR
C/1995 O1 (Hale-Bopp)	1997 March 28	0.92	3.33 ± 0.26	1.17 ± 0.13
C/1999 S4 (LINEAR)	2000 July 5	0.86	3.31 ± 0.10	1.16 ± 0.05
C/2001 A2 (LINEAR)	2001 July 27	1.39	3.47 ± 0.11	1.24 ± 0.06
153P/Ikeya-Zhang	2002 April 20	0.89	3.27 ± 0.10	1.14 ± 0.05
C/2000 WM ₁ (LINEAR)	2002 March 7	1.08	3.25 ± 0.07	1.13 ± 0.04
	2002 March 7	1.08	3.22 ± 0.09	1.11 ± 0.05
	2002 March 8	1.10	3.19 ± 0.10	1.10 ± 0.05
	2002 March 8	1.10	3.24 ± 0.11	1.12 ± 0.06
	2002 March 22	1.33	3.25 ± 0.12	1.13 ± 0.06
	2002 March 22	1.33	3.25 ± 0.08	1.13 ± 0.04
	2002 March 23	1.34	3.26 ± 0.10	1.13 ± 0.05
	2002 March 23	1.34	3.24 ± 0.11	1.12 ± 0.06
	2003 January 8	1.22	3.30 ± 0.08	1.15 ± 0.04
C/2002 V1 (NEAT)	2003 January 8	1.22	3.25 ± 0.11	1.13 ± 0.06
	2003 January 10	1.19	3.31 ± 0.10	1.16 ± 0.05
	2003 January 10	1.18	3.28 ± 0.10	1.14 ± 0.05
	2003 March 21	1.01	3.25 ± 0.09	1.13 ± 0.05
	2003 February 19	0.70	3.29 ± 0.08	1.15 ± 0.04
	2003 February 20	0.72	3.25 ± 0.13	1.13 ± 0.07
	2003 February 20	0.72	3.22 ± 0.14	1.11 ± 0.07
	2003 March 7	1.06	3.27 ± 0.09	1.14 ± 0.05
	2003 March 7	1.07	3.21 ± 0.10	1.11 ± 0.05
C/2002 Y1 (Juels-Holvorcem)	2003 May 29	1.14	3.25 ± 0.10	1.13 ± 0.05
	2003 May 29	1.14	3.27 ± 0.09	1.14 ± 0.05
	2003 May 30	1.16	3.24 ± 0.12	1.12 ± 0.06
	2003 May 30	1.16	3.19 ± 0.12	1.10 ± 0.06
	2004 April 18	1.37	3.39 ± 0.09	1.20 ± 0.05
	2004 April 19	1.37	3.42 ± 0.09	1.21 ± 0.05
	2004 April 20	1.37	3.35 ± 0.06	1.18 ± 0.03
	2004 April 22	1.37	3.41 ± 0.09	1.21 ± 0.05
	2004 May 2	1.39	3.41 ± 0.11	1.21 ± 0.06
88P/Howell	2004 May 3	1.39	3.37 ± 0.08	1.19 ± 0.04
	2004 May 4	1.39	3.31 ± 0.10	1.16 ± 0.05
	2004 May 17	1.42	3.45 ± 0.10	1.23 ± 0.05
	2004 May 21	1.43	3.45 ± 0.09	1.23 ± 0.05
	2004 May 22	1.44	3.36 ± 0.08	1.18 ± 0.04
	2004 May 24	1.44	3.31 ± 0.10	1.16 ± 0.05
	2004 May 5	0.98	3.25 ± 0.06	1.13 ± 0.03
	2004 May 5	0.98	3.20 ± 0.06	1.10 ± 0.03
	2004 May 5	0.98	3.22 ± 0.10	1.11 ± 0.05
C/2001 Q4 (NEAT)	2004 May 5	0.98	3.16 ± 0.16	1.08 ± 0.08
	2004 May 5	0.98	3.17 ± 0.14	1.09 ± 0.07
	2004 May 5	0.98	3.19 ± 0.18	1.10 ± 0.09
	2004 May 6	0.98	3.27 ± 0.10	1.14 ± 0.05
	2004 May 6	0.98	3.24 ± 0.17	1.12 ± 0.09
	2004 May 6	0.98	3.23 ± 0.19	1.12 ± 0.10
	2004 May 7	0.97	3.29 ± 0.08	1.15 ± 0.04
	2004 May 6	0.68	3.24 ± 0.09	1.12 ± 0.05
	2004 May 26	0.94	3.25 ± 0.11	1.13 ± 0.06
C/2002 T7 (LINEAR)	2004 May 27	0.94	3.28 ± 0.08	1.14 ± 0.04
	2004 November 20	1.20	3.32 ± 0.07	1.16 ± 0.04
	2005 July 2	1.51	3.25 ± 0.08	1.13 ± 0.04
	2005 July 3	1.51	3.25 ± 0.08	1.13 ± 0.04
	2005 July 4	1.51	3.24 ± 0.09	1.12 ± 0.05
	2005 July 5	1.51	3.32 ± 0.11	1.16 ± 0.06
	2005 July 6	1.51	3.31 ± 0.09	1.16 ± 0.05
	2005 July 7	1.51	3.27 ± 0.10	1.14 ± 0.05
	2005 July 8	1.51	3.33 ± 0.11	1.17 ± 0.06
C/2003 K4 (LINEAR)	2005 July 9	1.51	3.27 ± 0.10	1.14 ± 0.05
	2005 July 10	1.51	3.28 ± 0.12	1.14 ± 0.06
	2005 July 11	1.51	3.29 ± 0.10	1.15 ± 0.05
	2006 May 27	0.95	3.04 ± 0.06	1.02 ± 0.03
	2006 June 12	0.94	3.02 ± 0.06	1.01 ± 0.03
	2008 January 16	1.04	3.29 ± 0.06	1.15 ± 0.03
	2008 January 28	1.03	3.28 ± 0.08	1.14 ± 0.04
	2008 February 4	1.03	3.26 ± 0.09	1.13 ± 0.05

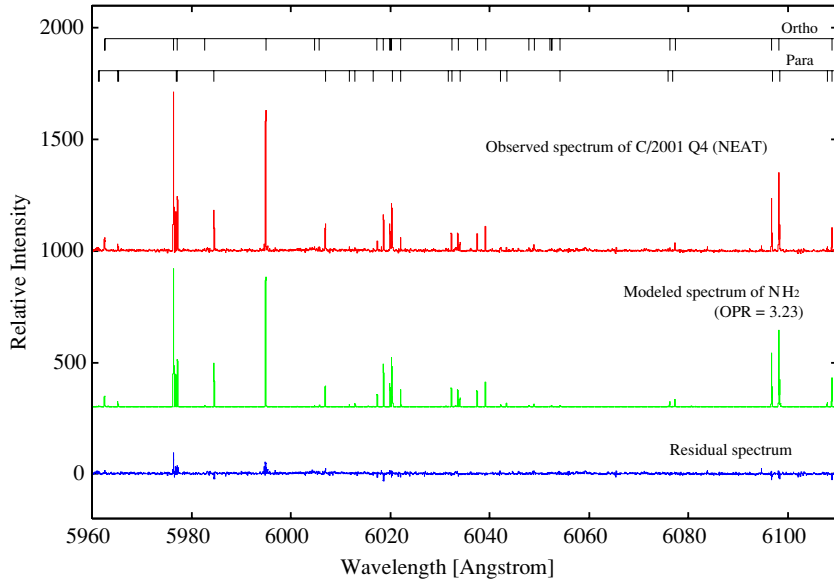


Figure 1. Comparison between observed and modeled (best-fit) spectra of NH_2 in C/2001 Q4 (NEAT). Observed and modeled spectra are with offsets of 1000 and 300, respectively. These spectra are in good agreement (the residual spectrum between them is also plotted in the figure). The ortho- and para- NH_2 lines are labeled in these spectra. Although the line intensity of the C_2 Swan band ($\Delta v = -2$) is much weaker than the NH_2 lines in the (0,9,0) band, many weak lines of C_2 are recognized in the residual spectrum (not noise).

(A color version of this figure is available in the online journal.)

Table 3
Ortho-to-Para Abundance Ratios of NH_3 and $^{14}\text{N}/^{15}\text{N}$ Ratios in CN for the Comets

Comet	OPR of NH_3	T_{spin} of NH_3 (K)	$^{14}\text{N}/^{15}\text{N}$ Ratio in CN	Orbital Period (yr)
C/1995 O1 (Hale-Bopp)	1.17 ± 0.13	$28 +12/-4$	143 ± 30^a	4000
C/1999 S4 (LINEAR)	1.16 ± 0.05	$28 +3/-2$	150 ± 50^b	Dynamically new
C/2001 A2 (LINEAR)	1.24 ± 0.06	25 ± 2	$\geq 60^c$	40000
153P/Ikeya-Zhang	1.14 ± 0.05	$29 +4/-2$	140 ± 50^d	365
C/2000 WM ₁ (LINEAR)	1.12 ± 0.02	30 ± 1	150 ± 30^e	Dynamically new
C/2002 V1 (NEAT)	1.14 ± 0.02	29 ± 1	160 ± 35^c	Young long period, 37000
C/2002 X5 (Kudo-Fujikawa)	1.13 ± 0.02	30 ± 1	130 ± 20^c	Dynamically new
C/2002 Y1 (Juels-Holvorcem)	1.13 ± 0.03	30 ± 2	150 ± 35^c	Old long period
88P/Howell	1.19 ± 0.02	27 ± 1	140 ± 20^b	5.5
C/2001 Q4 (NEAT)	1.12 ± 0.02	30 ± 1	135 ± 20^a	Dynamically new
C/2002 T7 (LINEAR)	1.13 ± 0.03	30 ± 2	160 ± 25^c	Dynamically new
C/2003 K4 (LINEAR)	1.16 ± 0.04	$28 +3/-2$	145 ± 25^c	Dynamically new
9P/Tempel 1	1.14 ± 0.02	29 ± 1	145 ± 25^f	5.5
73P-B/Schwassmann-Wachmann 3	1.01 ± 0.03	> 39	210 ± 50^g	5.4
73P-C/Schwassmann-Wachmann 3	1.02 ± 0.03	> 37	220 ± 40^g	5.4
8P/Tuttle	1.14 ± 0.02	29 ± 1	150 ± 30^h	13.6

References. ^a Manfroid et al. 2005; ^b Hutsemékers et al. 2005; ^c Manfroid et al. 2009; ^d Jehin et al. 2004; ^e Arpigny et al. 2003; ^f Jehin et al. 2006; ^g Jehin et al. 2008; ^h Jehin et al. 2009a.

T_{spin} for water (30 K) reported by Dello Russo et al. (2005). The depletion in highly volatile species in this comet might be the signature for formation in a warmer region than other typical comets. However, the T_{spin} of NH_3 determined in our study implies that the materials in this comet formed at an environment similar to others (see the discussion in Section 5). The T_{spin} may indicate formation conditions corresponding to the formation of molecules in the pre-solar molecular cloud while the chemical abundance ratio of cometary volatiles reflects the temperature at the accretion of cometary nuclei in the solar nebula.

4.3. Comet C/2001 A2 (LINEAR)

Comet C/2001 A2 (LINEAR) showed frequent outburst phenomena linked to fragmentations (e.g., Jehin et al. 2002).

Near-infrared spectroscopy revealed that the comet was enriched in organics (Magee-Sauer et al. 2008). We also reported the OPR of NH_3 in this comet as 1.25 ± 0.05 (Kawakita et al. 2004) while the revised value is OPR = 1.24 ± 0.06 corresponding to $T_{\text{spin}} = 25 \pm 2$ K for NH_3 . The NH_3 T_{spin} in this comet is relatively lower than the usual value of ~ 30 K and this conclusion is consistent with the water T_{spin} derived by Dello Russo et al. (2005) as 23_{-3}^{+4} K. These lower T_{spin} may be related to the organic-rich chemistry and frequent outbursts (with fragmentations) in this comet.

4.4. 153P/Ikeya-Zhang

Comet Ikeya-Zhang is now in a Halley-type orbit, and thus probably originated in the Oort Cloud. The OPR of NH_3 of this comet was reported to be 1.11 ± 0.06 (Kawakita et al. 2004)

while the revised value is 1.14 ± 0.05 (corresponding to $T_{\text{spin}} = 29_{-2}^{+4}$ K) in NH_3 . Improvement in the method of data analysis changes the results slightly but consistently with previous result. Comet Ikeya-Zhang is a typical comet from the viewpoint of T_{spin} .

4.5. C/2000 WM₁ (LINEAR)

The OPRs of NH_3 in comet C/2000 WM₁ (LINEAR) were determined based on multiple measurements of OPR of NH_2 (shown in Table 3). The weighted mean of the NH_3 OPR is 1.12 ± 0.02 in this comet. The corresponding T_{spin} of NH_3 is 30 ± 1 K. This is consistent with T_{spin} derived for water, OPR = 2.6 ± 0.2 corresponding to $T_{\text{spin}} \sim 31$ K (28–38 K; Radeva et al. 2010). This comet is also typical in T_{spin} .

4.6. C/2002 V1 (NEAT)

In comet C/2002 V1 (NEAT), the weighted mean of the NH_3 OPR is 1.14 ± 0.02 based on multiple observations of the comet (Table 3). The T_{spin} of NH_3 is 29 ± 1 K like other comets typical in T_{spin} .

4.7. C/2002 X5 (Kudo-Fujikawa)

Based on multiple observations of comet C/2002 X5 (Kudo-Fujikawa), we derived the weighted mean of the NH_3 OPR to be 1.13 ± 0.02 indicating $T_{\text{spin}} = 30 \pm 1$ K for NH_3 . This comet is also normal in T_{spin} .

4.8. C/2002 Y1 (Juels-Holvorcem)

In comet C/2002 Y1 (Juels-Holvorcem), the weighted mean of the NH_3 OPR is 1.13 ± 0.03 (corresponding to $T_{\text{spin}} = 30 \pm 2$ K) based on multiple observations. The derived OPR of NH_3 is in the typical range.

4.9. 88P/Howell

This comet belongs to the Jupiter family comets (JFCs). It was observed at multiple epochs and the determinations of the NH_3 OPR led to the weighted mean value of OPR = 1.19 ± 0.02 ($T_{\text{spin}} = 27 \pm 1$ K) for NH_3 . Since the T_{spin} of this comet is similar to those for the Oort Cloud comets (~ 30 K, see above), icy materials incorporated in the comets now in different reservoirs (the Oort Cloud and the Kuiper Belt) might be formed in similar environments.

4.10. C/2001 Q4 (NEAT)

Comet C/2001 Q4 (NEAT) was observed many times and we derived OPRs of NH_3 for each observation. The weighted mean of the NH_3 OPR is 1.12 ± 0.02 ($T_{\text{spin}} = 30 \pm 1$ K) based on the observations with VLT/UVES. In our previous study (Kawakita et al. 2006), the NH_3 OPR = 1.11 ± 0.04 and $T_{\text{spin}} = 31_{-2}^{+4}$ K were derived from the Subaru/HDS observation. These values have been revised recently by Shinnaka et al. (2010), as OPR = 1.12 ± 0.02 and $T_{\text{spin}} = 30 \pm 1$ K. These OPRs of NH_3 based on the Subaru/HDS observations are consistent with the OPRs derived from the VLT/UVES observations in this work. Furthermore, T_{spin} of water and methane was also derived from the near-infrared high-dispersion spectrum (Kawakita et al. 2005, 2006). All these T_{spin} values (31_{-5}^{+11} K for water, 30_{-1}^{+2} K for NH_3 , and 33_{-1}^{+2} K for methane) are consistent with one another in this comet.

4.11. C/2002 T7 (LINEAR)

In the case of comet C/2002 T7 (LINEAR), we report the OPR of NH_3 as 1.13 ± 0.03 corresponding to $T_{\text{spin}} = 30 \pm 2$ K. This value seems typical of our sample. In this comet, the D/H ratio in OH (photodissociation product of H_2O) is also measured and the typical D/H ratio in water was obtained ($\sim 3 \times 10^{-4}$) by Hutsemékers et al. (2008).

4.12. C/2003 K4 (LINEAR)

The OPR of NH_3 in comet C/2003 K4 (LINEAR) is 1.16 ± 0.04 . The resultant T_{spin} of NH_3 is 28_{-2}^{+3} K. This temperature is consistent with T_{spin} in other comets and also consistent with the T_{spin} of water ($28.5_{-3.5}^{+6.5}$ K) derived by Woodward et al. (2007) based on infrared observations.

4.13. 9P/Tempel 1

Comet 9P/Tempel 1 is a JFC and was the target of the NASA Deep Impact mission (A'Hearn et al. 2005). Although the data were analyzed and already published by Kawakita et al. (2007), we revisited the data and used the improved method for this comet. Since this comet is dust-rich in the optical spectra, precise subtraction of the solar continuum would improve the results. We report the OPR of NH_3 as 1.14 ± 0.02 (weighted mean of multiple observations), which is lower than previous values. The T_{spin} of NH_3 is 29 ± 1 K for 9P/Tempel 1 while it is ~ 25 K in our previous report (Kawakita et al. 2007). Relatively high dust-to-gas ratio in this comet would be the reason for this change (see the case of C/Hale-Bopp). However, the basic conclusion has not changed; namely, no significant change in the OPR of NH_3 was found before and after the Deep Impact on 2005 July 4 (see Figure 2). In Figure 2, we plotted the obtained OPRs with random errors (not including systematic ones) to check the change in OPR before and at the Deep Impact. Based on this figure, we conclude that the OPRs did not change after the Deep Impact event with the confidence level of 95%. Anyway, comet 9P/Tempel 1 is similar to Oort Cloud comets (and also similar to 88P/Howell as a JFC) from the viewpoint of T_{spin} in our sample.

4.14. 73P/Schwassmann-Wachmann 3 (B- and C-fragments)

Comet 73P/Schwassmann-Wachmann 3 is a very peculiar comet that showed fragmentation into many fragments. In the 2006 apparition, it was expected that the fresh icy materials exposed on the new surface (formed by the fragmentations) could be observed. Comparison of the chemistry between the main fragments B and C implies that the parent body was homogeneous in chemistry (Biver et al. 2008; Villanueva et al. 2006; Dello Russo et al. 2007; Kobayashi et al. 2007; Schleicher & Bair 2008). Jehin et al. (2009a) pointed out that the parent comet is peculiar from the viewpoint of the $^{14}\text{N}/^{15}\text{N}$ ratio in CN and OPR of NH_3 . We reanalyzed the data and found OPR = 1.01 ± 0.03 and 1.02 ± 0.03 for fragments B and C, respectively. These values are far from the typical values in our sample and consistent with the high-temperature limit (1.0) for NH_3 . The nuclear spin temperatures are higher than 39 K and 37 K for fragments B and C, respectively. These signatures for high temperatures are consistent with the results derived for water. The lower limits of T_{spin} of water are reported as 42 K and 37 K for the B- and C-fragments (Dello Russo et al. 2007). These results may be related to the strong depletion in highly volatile species (Villanueva et al. 2006; Dello Russo et al.

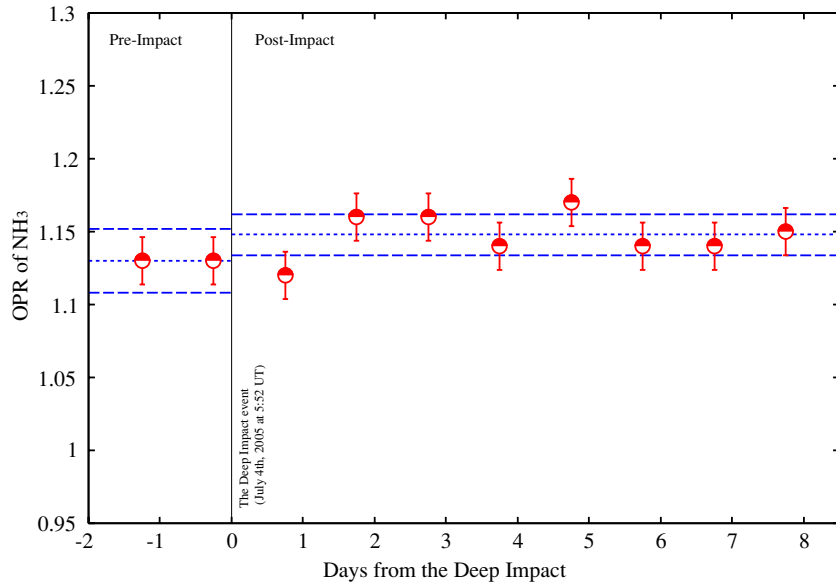


Figure 2. Temporal variation of OPRs of NH_3 in comet 9P/Tempel 1 before and after the Deep Impact. We plotted the NH_3 OPRs with their random errors in each measurement and the error bars correspond to $\pm 1\sigma$ error levels. The dotted and dashed lines show mean values and a 95% confidence level of the mean for before and after the impact (1.130 ± 0.022 and 1.147 ± 0.014), respectively. These values overlap within their 95% confidence levels. The disagreement between before and after impact is not significant.

(A color version of this figure is available in the online journal.)

2007; Kobayashi et al. 2007). We will discuss the peculiarity of 73P/Schwassmann-Wachmann 3 in Section 5.

4.15. 8P/Tuttle

Comet 8P/Tuttle is now classified as a Halley-type comet, and thus probably comes from the Oort Cloud. The weighted mean of the OPR for NH_3 is 1.14 ± 0.02 (corresponding to 29 ± 1 K). This is similar to the other Halley-type comet in our sample, comet 153P/Ikeya-Zhang (and similar to most comets in our database). Our determination of the OPR of NH_3 indicates that comet 8P/Tuttle is a typical comet. Near-infrared spectroscopic observations revealed that the chemical composition of 8P/Tuttle is slightly different from that of typical Oort Cloud comets (Bonev et al. 2008a; Kobayashi et al. 2010). However, the D/H ratio in water (considered as a sensitive indicator of the temperatures where the molecules formed) is similar to those found in other Oort Cloud comets (Villanueva et al. 2008).

5. DISCUSSION AND CONCLUSION

5.1. Ortho-to-para Abundance Ratio of Cometary NH_3

Figure 3 (OPRs versus heliocentric distances at the observations) and Figure 4 summarize the results of this work. As clearly shown in these figures, the OPRs of NH_3 show a cluster between 1.1 and 1.2 in our data set. These values correspond to ~ 30 K as T_{spin} . Note that the fragments (B and C) of comet 73P/Schwassmann-Wachmann 3 (hereafter, 73P/SW3) seem to be peculiar objects showing OPRs consistent with the high-temperature limit for NH_3 (1.0). Their error bars are small enough to distinguish the comet 73P/SW3 from other comets. Comet 73P/SW3 is also showing a peculiar $^{14}\text{N}/^{15}\text{N}$ ratio measured in the CN radical (Jehin et al. 2008). We discuss the relationship between OPRs of NH_3 and $^{14}\text{N}/^{15}\text{N}$ ratios later.

First of all, we checked the relationship between the OPRs of NH_3 and the heliocentric distances when the comets were

observed (Figure 3 and Table 2). Limbach et al. (2006) proposed that OPRs are diagnostics for the temperatures of the surface of cometary nuclei based on their theoretical studies. In this case, the OPRs should depend on the distances from the Sun at the observations since the surface temperature depends on the distance from the Sun (i.e., warmer when closer to the Sun). If we consider the blackbody approximation for the surface temperature of the nucleus, the temperature is expected to be $280/\sqrt{r}$ (K) at r (AU) from the Sun. Temperatures could vary by a factor of ~ 1.5 within the range of heliocentric distance from 0.7 to 1.5 AU. However, the OPRs determined in our data set did not depend on the heliocentric distances at the observations (at least, in the range from 0.7 to 1.5 AU from the Sun) as shown in Figure 3. Such a trend was also found in our previous study (Kawakita et al. 2004) and also discussed by Crovisier (2006, 2007). Therefore, the OPRs probably do not reflect the temperatures of the nucleus surface.

Cacciani et al. (2009) recently calculated the nuclear spin conversion rate of NH_3 in the gas phase based on a quantum relaxation model. The conversion between ortho and para species may also be possible by proton-exchange reactions in the coma (Irvine et al. 2000). In such cases, the nuclear spin temperatures might equilibrate with the kinetic temperatures of the gas in the coma. However, the OPRs determined in our data set are almost constant for the comets with different gas production rates at different heliocentric distances. Since the kinetic temperature of gas in the coma depends on both the heliocentric distance (i.e., the total energy input to the comet from the Sun) and the total gas production rate (the gas in the coma would be heated up by the hot photodissociation products of parent molecules like water), our results imply that the OPRs are nearly constant for different kinetic temperatures of the gas in the coma. Furthermore, the OPRs of water and NH_2 were observed to be constant with distances from the nucleus in the coma for a few comets in the previous studies (Kawakita et al. 2004; Bonev et al. 2007, 2008a). It is unlikely that ortho and para species were interchanged in the coma.

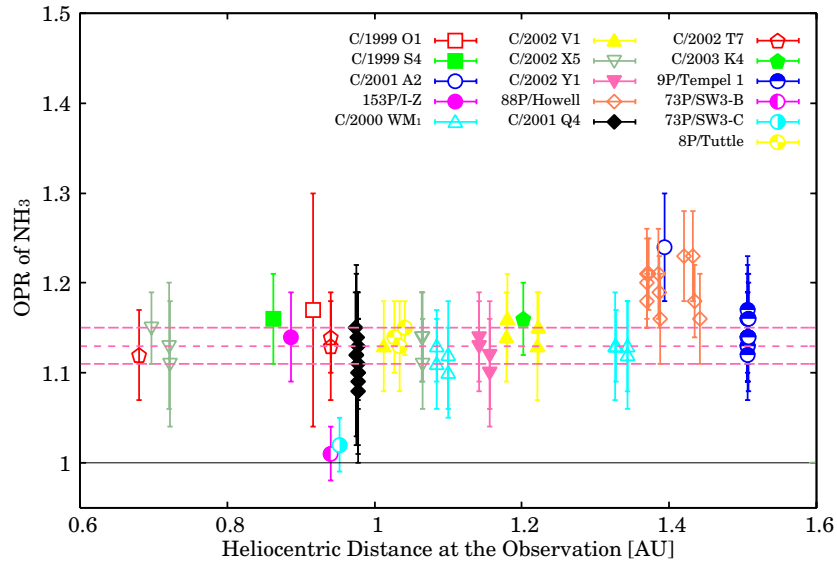


Figure 3. Relationship between OPRs of NH_3 and heliocentric distances at the observations. The weighted mean value of the OPR of cometary NH_3 in 15 comets is 1.13 ± 0.02 (pink dot and dash lines). The black bar shows the nuclear spin statistical weight ratio of ammonia (1.0). There is no correlation between the NH_3 OPRs and heliocentric distances at the observations. Therefore, OPRs may not be reflecting the kinetic temperature of NH_3 .

(A color version of this figure is available in the online journal.)

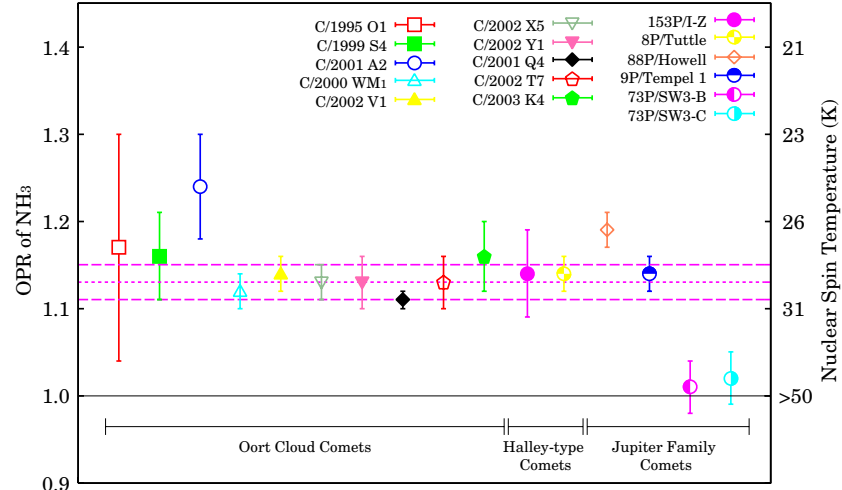


Figure 4. OPRs of NH_3 in comets (if multiple observations were carried out for a given comet, we show the weighted mean OPR). The dashed lines and dotted lines are the weighted mean value and $\pm 1\sigma$ levels for all measurements shown here. Both the OPRs and T_{spin} of ammonia show a cluster between 1.1 and 1.2 and 30 K for all comets in our sample, except for 73P/SW3, respectively. Comet 73P/SW3 (both B- and C-fragments) shows the OPR of ammonia consistent with the nuclear spin statistical weight ratio (1.0) that indicates a high-temperature limit as T_{spin} .

(A color version of this figure is available in the online journal.)

The possibility that the OPRs of NH_3 equilibrated with the internal temperatures of the cometary nuclei (Mumma et al. 1993) is re-examined here. According to theoretical studies (e.g., Rosenberg & Prialnik 2007; Prialnik et al. 2004; Podolak & Prialnik 1996) the internal temperature at a depth of several meters or deeper is almost constant. Therefore, the OPR might equilibrate with such an internal temperature over a long time. Based on Table 3, however, there is no clear relationship between OPRs and orbital periods, as already pointed out in the previous studies (Irvine et al. 2000; Kawakita et al. 2004; Crovisier 2007). At least, it seems unlikely that all comets discussed here (their orbital periods span the range from ~ 5 to longer than 10^4 yr) have internal temperatures near 30 K. Our results imply that the OPRs are not related to the internal temperatures of the cometary nuclei.

On the other hand, from the viewpoint of the dynamical origin of the comets, the OPR of cometary NH_3 does not depend on the

dynamical reservoirs of comets (the Oort Cloud or the Kuiper Belt) as shown in Figure 4. Different dynamical reservoirs originated in different regions of the solar nebula (although the cometary birth places for the different reservoirs might be partly overlapping with each other, as proposed by the Nice model; see Morbidelli 2008), and therefore, it appears that OPRs are not related to the physical conditions in the solar nebula.

If OPRs equilibrated with the temperatures where comets formed (from 5 to 30 AU from the Sun) in the solar nebula, the nuclear spin temperatures would vary by a factor of ~ 2 or more based on the modeled temperature profile of the solar nebula (Boss 2001; Hersant et al. 2001; Jang-Condell 2008; Willacy et al. 1998) while the obtained nuclear spin temperatures are nearly constant, ~ 30 K. We then conclude that the OPR of NH_3 reflects an old memory before cometary formation in the solar nebula (except for comet 73P/SW3). The OPRs of NH_3 probably reflect the processes and physical conditions prevailing

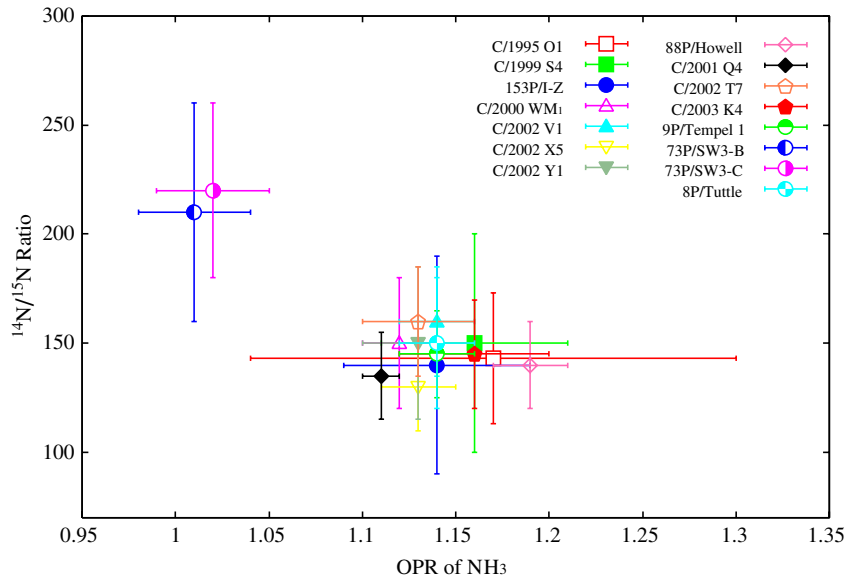


Figure 5. Relationship between $^{14}\text{N}/^{15}\text{N}$ ratios in CN and NH_3 OPRs. Most comets show similar OPRs (1.1–1.2) and similar $^{14}\text{N}/^{15}\text{N}$ ratios (~ 140) except for comet 73P/SW3. Comet 73P/SW3 is clearly distinguished from other comets in this plot. Based on this figure, it is likely that both the OPR of NH_3 and the $^{14}\text{N}/^{15}\text{N}$ ratio in CN reflect the same environment at molecular formation. There may be two distinct groups of comets in this plot. This figure is based on Table 3.

(A color version of this figure is available in the online journal.)

during the molecular formation in the pre-solar molecular cloud. Cometary ammonia (and probably also water) formed on cold grains at ~ 30 K in the pre-solar molecular cloud. The comet 73P/SW3, which is an exception to this scenario, will be discussed in Section 5.3.

5.2. Comparison of Ammonia OPRs with Other Properties

The relationship between the OPRs of NH_3 and the $^{14}\text{N}/^{15}\text{N}$ ratios in CN is the most interesting result as shown in Figure 5 and Table 3. Most comets show similar OPRs (1.1–1.2) and similar $^{14}\text{N}/^{15}\text{N}$ ratios (~ 140) except for comet 73P/SW3. Comet 73P/SW3 is clearly distinguished in the plot of the OPR of NH_3 versus the $^{14}\text{N}/^{15}\text{N}$ ratio in CN. Based on this result, there may be some link between the OPR of NH_3 and the $^{14}\text{N}/^{15}\text{N}$ ratio in CN. There may be two distinct groups of comets in the plot as shown in Figure 5. Boney et al. (2008a) also pointed out the existence of two groups based on water OPRs. Such a classification is very curious for the comet's taxonomy. Figure 5 may imply that the molecules in cometary ice formed in similar environments for most comets. Since comet 73P/SW3 shows NH_3 OPRs of 1.0 (a high-temperature limit) and a higher $^{14}\text{N}/^{15}\text{N}$ ratio in CN (lower fractionation in ^{15}N) than other comets, these facts indicate that the materials incorporated in comet 73P/SW3 formed under relatively warmer conditions than most comets.

Please note that it is hard to explain the observed $^{14}\text{N}/^{15}\text{N}$ ratios (~ 140) under cold temperatures (~ 30 K) estimated from the observed OPRs of NH_3 (1.1–1.2) as T_{spin} . The $^{14}\text{N}/^{15}\text{N}$ ratios in HCN (which is likely a major parent of CN in cometary coma) in the gas phase were determined to be in the range 200–600 by radio observations of pre-protostellar cores with kinetic temperatures of 6–10 K (Hily-Blant et al. 2010). These values are higher than the $^{14}\text{N}/^{15}\text{N}$ ratios found in comets (~ 140). Such a high fractionation of ^{15}N in comets is also found in interplanetary dust particles (IDPs) in our solar system (Messenger et al. 2003). The model for ^{15}N fractionation in nitriles could explain the discrepancy in interstellar chemistry at low temperatures proposed by Rodgers & Charnley (2008a).

The authors claimed that super-fractionation for the solid-phase isotopologues of nitriles occurs under low-temperature conditions (~ 7 K). However, this temperature is inconsistent with nuclear spin temperatures of NH_3 in comets.

This fact may indicate that (1) physical temperatures estimated as nuclear spin temperatures are not appropriate, or (2) there might be other mechanisms to achieve the fractionation of ^{15}N in the parent molecules of CN (HCN) at temperatures under ~ 30 K. Regarding case (1), we usually refer to the rotational energy levels of isolated NH_3 in space. We may have to refer to the rotational energy diagram of NH_3 on the grain where the molecules formed and its OPR was fixed, as pointed out by Crovisier (2007). However, the rotational energy structure for NH_3 physisorbed on the grain is expected to be not so different from the case of isolated NH_3 . When we assume the isolated molecules for the calculation of T_{spin} , water and methane as well as ammonia indicate similar T_{spin} in each comet (Figure 6). This fact may indicate that those molecules physisorbed on cold grains at their formation.

Furthermore, the temperature of grains might not be the same as the temperature of the surrounding gas in diffuse cloud environments (they might not be in thermal equilibrium). NH_3 is considered to be formed on cold grain surface efficiently while HCN (as a parent of CN in cometary coma) could be formed in gas phase efficiently (Rodgers & Charnley 2008b). Therefore, both OPRs of NH_3 and $^{14}\text{N}/^{15}\text{N}$ ratios in CN might not indicate the same temperature. Otherwise, NH_3 and HCN formed at different epochs (e.g., at different temperatures) even in the same molecular cloud or in the solar nebula. In any case, future determination of $^{14}\text{N}/^{15}\text{N}$ in NH_3 is quite essential to get more information on the relationship between OPRs and $^{14}\text{N}/^{15}\text{N}$ in cometary materials (Charnley & Rodgers 2008).

The D/H ratio in cometary molecules also reflects the conditions at the time of molecular formation in the early solar system. The D/H ratio is a powerful tool for investigating the formation temperature of molecules in the pre-solar molecular cloud or the solar nebula, especially under low-temperature conditions. However, the number of comets in which the

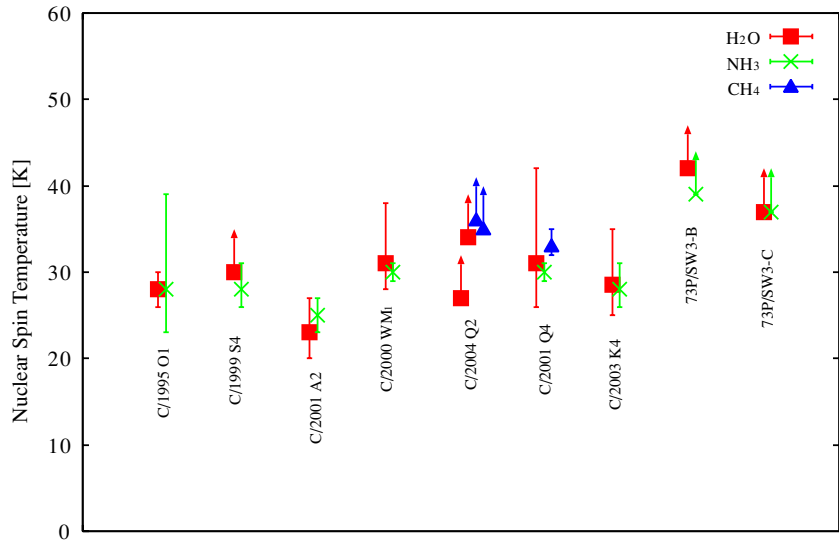


Figure 6. Comparison among T_{spin} of H_2O , NH_3 , and CH_4 . Water and methane as well as ammonia indicate consistent T_{spin} in each comet. This fact may indicate that those molecules equilibrated with cold grains at ~ 30 K. They might physisorb on the cold grains at their formation (see the text). References: C/1995 O1 (Crovisier et al. 1997), C/1999 S4 (Dello Russo et al. 2005), C/2001 A2 (Dello Russo et al. 2005), C/2000 WM₁ (Radeva et al. 2010), C/2004 Q2 (Bonev et al. 2007, 2009; Kawakita & Kobayashi 2009), C/2001 Q4 (Kawakita et al. 2006), C/2003 K4 (Woodward et al. 2007), 73P/SW3-B and -C (Bonev et al. 2007).

(A color version of this figure is available in the online journal.)

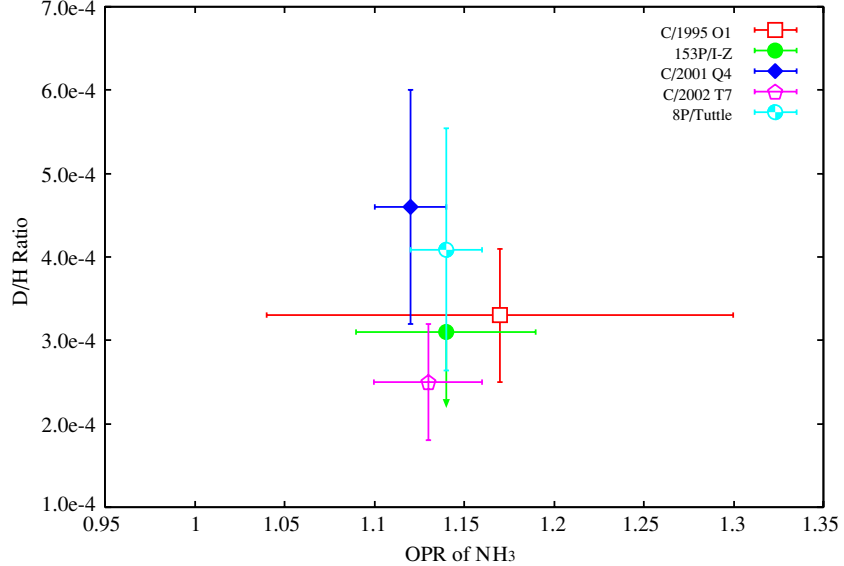


Figure 7. Relationship between D/H ratios in water and NH_3 OPRs. The D/H ratio in cometary molecules also reflects the conditions at the time of molecular formation in the early solar system. The D/H ratio in water is almost the same in all the comets observed so far, and the comets showing similar D/H ratios also show similar OPRs of NH_3 . This result also supports the hypothesis that the OPRs of NH_3 reflect the primordial conditions in the early solar system. References: C/1995 O1 (Meier et al. 1998), 153P/Ikeya-Zhang (Biver et al. 2006), C/2001 Q4 (Weaver et al. 2008), C/2002 T7 (Hutsemékers et al. 2009), 8P/Tuttle (Villanueva et al. 2009).

(A color version of this figure is available in the online journal.)

D/H ratios of water were determined is quite limited. Note that the D/H ratio is different for different molecular species; here we concentrate on the D/H ratio in water. The D/H ratios in water are about the same in all the comets observed so far, and the comets showing similar D/H ratios also show similar OPRs of NH_3 , as shown in Figure 7. This result also supports the hypothesis that the OPRs of NH_3 reflect a primordial information. But we clearly need more data for the D/H ratio in water to go further.

We also investigate the relationship between the mixing ratios of CO , CH_4 , C_2H_2 , C_2H_6 , HCN , CH_3OH , and NH_3 with respect to H_2O and the OPRs of NH_3 in comets (Figures 8–14).

Specifically, the sublimation temperatures of CO and CH_4 are around 30 K and their mixing ratios may be related to the OPRs ($T_{\text{spin}} \sim 30$ K). The mixing ratios of seven molecular species exhibit variety in the chemistry of the comets although the OPRs of NH_3 are almost constant in our samples. There are no clear correlations in those figures. The mixing ratios might reflect the surrounding environment where planetesimals formed or where cometary ices condensed from the gas phase in the solar nebula. Alternatively, hyper-volatiles like CO and CH_4 might sublimate from the icy grains, and these icy grains accreted to cometary nuclei under warmer conditions in the solar nebula.

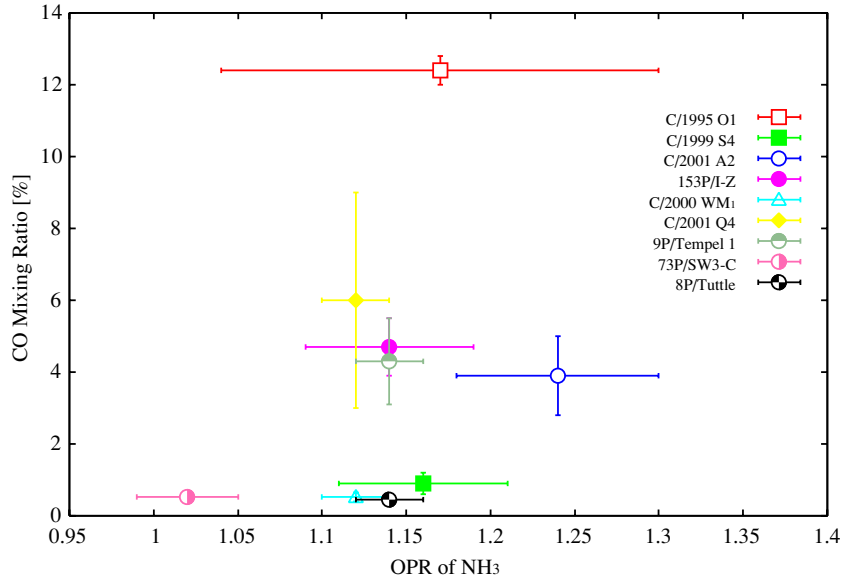


Figure 8. Relationship between NH_3 OPRs and CO mixing ratios (the sublimation temperature $T_{\text{subl}} = 25$ K in the early solar nebula; Meech & Svoren 2004). Note that T_{subl} is close to the T_{spin} of NH_3 obtained for many comets (~ 30 K). The CO mixing ratios exhibit variety in the chemistry of the comets although the OPRs of NH_3 are nearly constant in our samples. The CO mixing ratios probably reflect different environments (and/or different epochs) from that reflected by the OPR of NH_3 . Otherwise, the CO mixing ratio might be very sensitive to the temperature at the ice formation in the early solar nebula. References: C/1995 O1 (DiSanti et al. 2001), C/1999 S4 (Mumma et al. 2003), C/2001 A2 (Magee-Sauer et al. 2008), 153P/Ikeya-Zhang (Mumma et al. 2003), C/2000 WM₁ (Mumma et al. 2003), C/2001 Q4 (Combi et al. 2009), 9P/Tempel 1 (Mumma et al. 2005), 73P/SW3-C (DiSanti et al. 2007), and 8P/Tuttle (Böhnhardt et al. 2008).

(A color version of this figure is available in the online journal.)

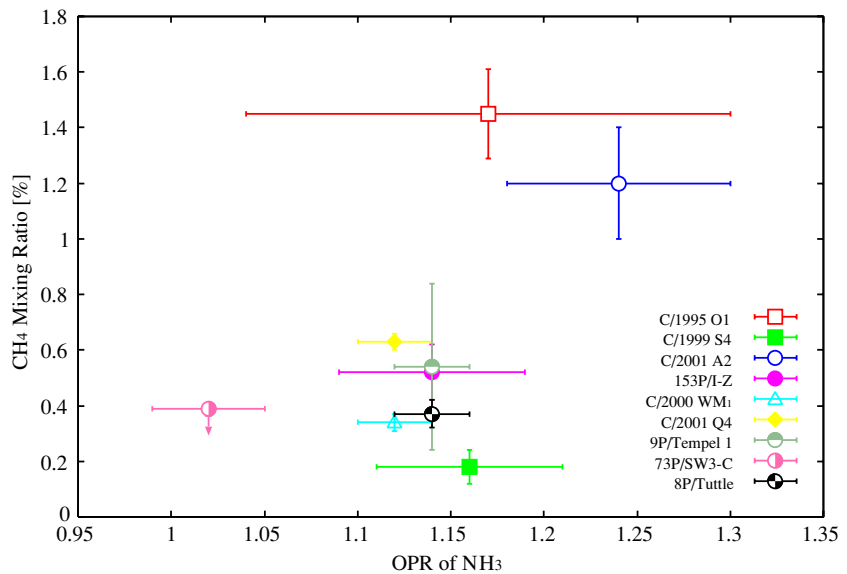


Figure 9. Relationship between NH_3 OPRs and CH_4 mixing ratios ($T_{\text{subl}} = 31$ K). The CH_4 mixing ratios also exhibit variety in the chemistry of the comets although the OPRs of NH_3 are nearly constant in our samples. As in the case of the CO mixing ratio, different environments might be reflected by CH_4 mixing ratios and the OPR of NH_3 . References: C/1995 O1 (Mumma et al. 2003), C/1999 S4 (Mumma et al. 2005), C/2001 A2 (Gibb et al. 2007), 153P/Ikeya-Zhang (Kawakita et al. 2003), C/2000 WM₁ (Radeva et al. 2010), C/2001 Q4 (Onishi et al. 2008), 9P/Tempel 1 (Mumma et al. 2005), 73P/SW3-C (Villanueva et al. 2006), and 8P/Tuttle (Böhnhardt et al. 2008; Bonev et al. 2008b).

(A color version of this figure is available in the online journal.)

5.3. Peculiarity of Comet 73P/Schwassmann-Wachmann 3 (B- and C-fragments)

We next consider the peculiar nature of comet 73P/SW3 in Figure 5. As pointed out in previous studies, comet 73P/SW3 shows not only peculiar OPRs of both H_2O and NH_3 but also peculiar chemical compositions of ice (Bonev et al. 2008a; Dello Russo et al. 2007; Jehin et al. 2008; Kobayashi et al. 2007). The depletion in hyper-volatiles and the nuclear spin temperatures

of both H_2O and NH_3 that are higher in the case of comet 73P/SW3 than in typical comets suggest that comet 73P/SW3 formed in a warmer region of the solar nebula (Jehin et al. 2008; Kobayashi et al. 2007). High $^{14}\text{N}/^{15}\text{N}$ ratio in CN also supports this hypothesis.

Several scenarios could be proposed for the peculiar OPRs in comet 73P/SW3. As a first scenario, comet 73P/SW3 might form from icy grains re-condensed in a relatively warmer region of the solar nebula. The temperatures in the solar nebula became

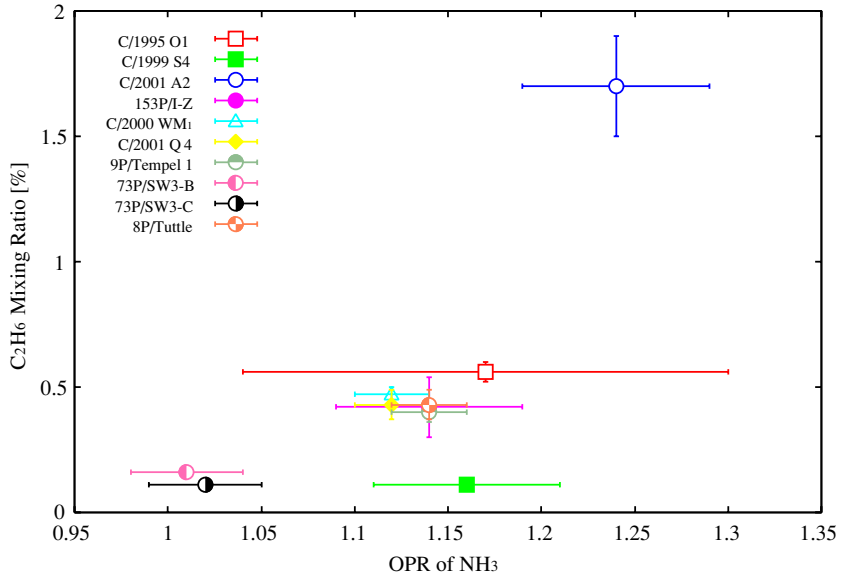


Figure 10. Relationship between NH₃ OPRs and C₂H₆ mixing ratios ($T_{\text{subl}} = 44$ K). Since T_{subl} is higher than the T_{spin} obtained for the comets (~ 30 K) and OPRs of NH₃ are nearly constant in our sample, little variation in the mixing ratios of C₂H₆ relative to H₂O is expected if T_{spin} indicates the temperature condition during ice formation in the early solar nebula. The C₂H₆ mixing ratios, however, also exhibit variety in the chemistry of the comets although the OPRs of NH₃ are nearly constant in our samples. No clear correlation is found between them. References: C/1995 O1 (Dello Russo et al. 2001), C/1999 S4 (Mumma et al. 2003), C/2001 A2 (Magee-Sauer et al. 2008), 153P/Ikeya-Zhang (Kawakita et al. 2003), C/2000 WM₁ (Radeva et al. 2010), C/2001 Q4 (Onishi et al. 2008), 9P/Tempel 1 (DiSanti et al. 2007), 73P/SW3-B and -C (Dello Russo et al. 2007), and 8P/Tuttle (Kobayashi et al. 2010).

(A color version of this figure is available in the online journal.)

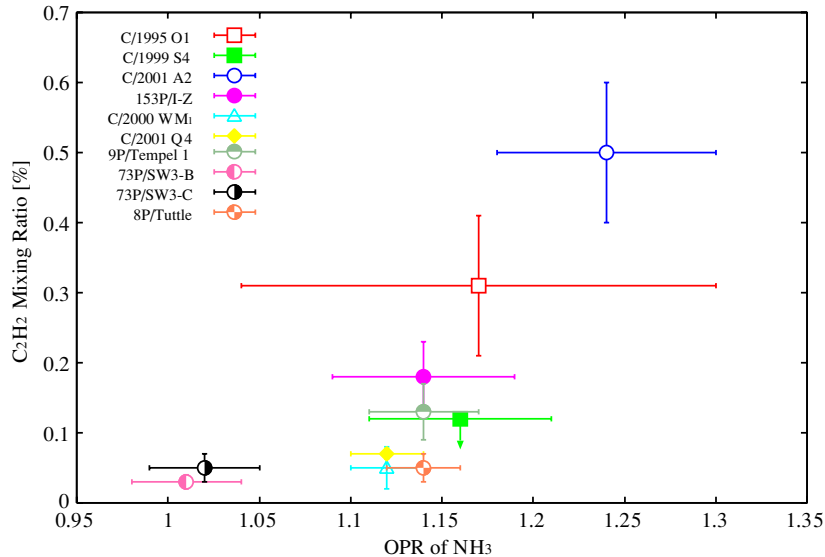


Figure 11. Same as Figure 10, but for C₂H₂ mixing ratios ($T_{\text{subl}} = 57$ K). References: C/1995 O1 (Magee-Sauer et al. 2001), C/1999 S4 (Mumma et al. 2003), C/2001 A2 (Magee-Sauer et al. 2008), 153P/Ikeya-Zhang (Mumma et al. 2003), C/2000 WM₁ (Radeva et al. 2010), C/2001 Q4 (Onishi et al. 2008), 9P/Tempel 1 (Mumma et al. 2005), 73P/SW3-B and -C (Dello Russo et al. 2007), and 8P/Tuttle (Kobayashi et al. 2010).

(A color version of this figure is available in the online journal.)

colder as the mass-accretion rate from the surrounding envelope of the solar nebula became smaller. Icy grains falling onto the solar nebula were once evaporated by the infall shock in the inner region (within ~ 30 AU; Lunine et al. 1991) and chemical reactions could occur in the gas phase. OPRs of molecules could be modified by those reactions (e.g., proton-exchange reactions). Thus, the re-condensed icy grains from the chemically altered materials in the solar nebula may indicate the signature of higher temperatures.

As a second scenario, the warming-up by radioactive nuclei in the interior of cometary materials may be another explanation

for the observational results. Since we observed the fragments of comet 73P/SW3, fresh ices (typical of the nucleus interior) might be exposed on their surface in this case. Because of the decay of ²⁶Al (Grimm & McSween 1993), the interior was heated up after the comet formation and both the OPR and ¹⁴N/¹⁵N ratios might have been reset in the interior while icy materials were not altered in other parts (near the surface) of the cometary nuclei. However, we could not find any mechanisms to achieve such alterations of both OPR and ¹⁴N/¹⁵N ratio. Observations of other break-up comets in the future may support this scenario.

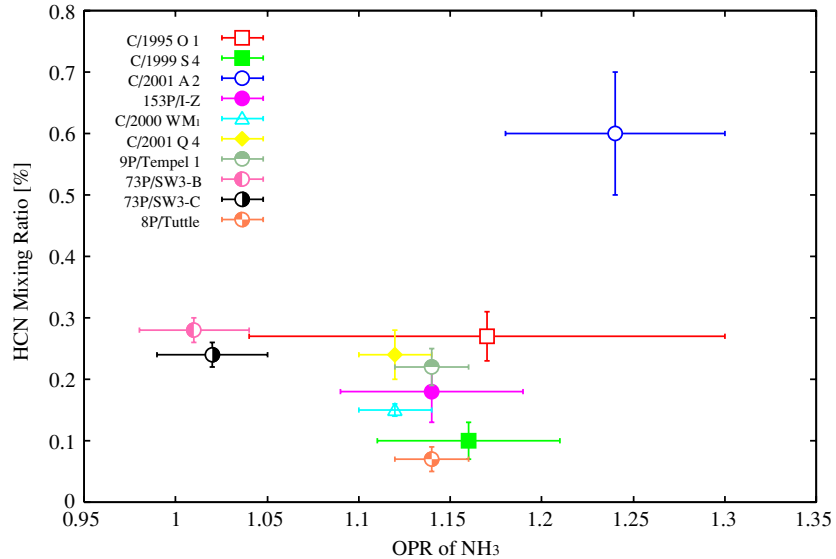


Figure 12. Same as Figure 10, but for HCN mixing ratios ($T_{\text{subl}} = 95$ K). References: C/1995 O1 (Magee-Sauer et al. 2001), C/1999 S4 (Bockelée-Morvan et al. 2001), C/2001 A2 (Magee-Sauer et al. 2008), 153P/Ikeya-Zhang (Magee-Sauer et al. 2002), C/2000 WM₁ (Radeva et al. 2010), C/2001 Q4 (Onishi et al. 2008), 9P/Tempel 1 (Mumma et al. 2005), 73P/SW3-B and -C (Dello Russo et al. 2007), and 8P/Tuttle (Kobayashi et al. 2010).

(A color version of this figure is available in the online journal.)

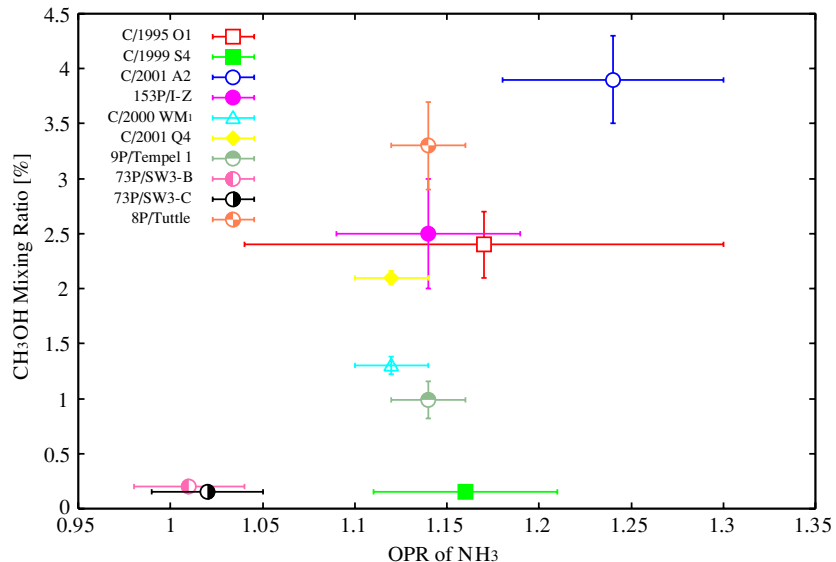


Figure 13. Same as Figure 10, but for CH₃OH mixing ratios ($T_{\text{subl}} = 99$ K). References: C/1995 O1 (Biver et al. 1999), C/1999 S4 (Mumma et al. 2003), C/2001 A2 (Magee-Sauer et al. 2008), 153P/Ikeya-Zhang (Mumma et al. 2003), C/2000 WM₁ (Radeva et al. 2010), C/2001 Q4 (Onishi et al. 2008), 9P/Tempel 1 (Mumma et al. 2005), 73P/SW3-B and -C (Dello Russo et al. 2007), and 8P/Tuttle (Kobayashi et al. 2010).

(A color version of this figure is available in the online journal.)

We would like to note the difference between comets C/1999 S4 (LINEAR) and 73P/SW3. As we already discussed in Section 4.2, comet C/1999 S4 (LINEAR) was depleted in organic volatiles but the T_{spin} of both H₂O and NH₃ is within the typical range, as well as the $^{14}\text{N}/^{15}\text{N}$ ratio in CN. On the other hand, both the OPRs and the $^{14}\text{N}/^{15}\text{N}$ ratios are out of the typical range in the case of comet 73P/SW3 (Figure 5) which is also depleted in the volatiles. This discrepancy may be explained by the chemical alteration of cometary materials in the warm region of the solar nebula. Most comets are thought to consist of icy materials formed in the pre-solar molecular cloud. Some highly volatile species might evaporate partially before the icy grains were incorporated into the comet, modifying the chemical composition. In addition, the icy materials incorporated into

comet 73P/SW3 might have condensed from the molecular gas in which gas-phase chemistry had changed OPRs and $^{14}\text{N}/^{15}\text{N}$ ratios.

5.4. Summary

We present OPRs of NH₃ in 15 comets based on high-dispersion spectra of the NH₂ (0,9,0) band in the optical range. The NH₃ OPR of comets in our sample shows a cluster between 1.1 and 1.2 (~ 30 K as T_{spin}) except for comet 73P/SW3. Both B- and C-fragments of this comet showed ammonia OPRs consistent with the nuclear spin statistical weight ratio (1.0) indicative of the high-temperature limit. Comparisons between OPRs of NH₃ and other properties ($^{14}\text{N}/^{15}\text{N}$ ratios in CN, D/H ratios of water, and mixing ratios of volatiles) are explored.

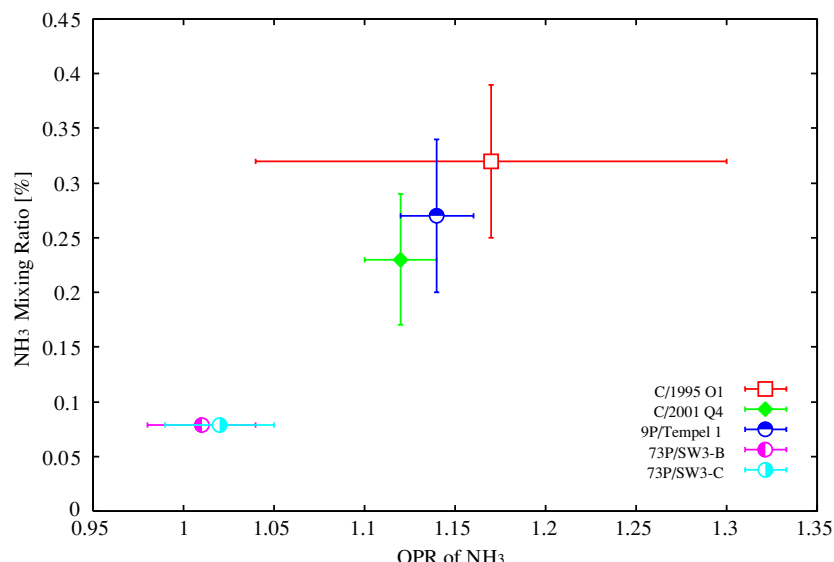


Figure 14. Same as Figure 10, but of NH_3 mixing ratios ($T_{\text{subl}} = 78$ K). The NH_3 mixing ratios are estimated from $\text{NH}_2/\text{H}_2\text{O}$ ratios obtained in optical spectroscopic observations (Fink 2009) based on the photodissociation branching ratio of NH_3 to NH_2 (0.95). In this plot, there may be the correlation between OPRs of NH_3 and NH_3 mixing ratios.

(A color version of this figure is available in the online journal.)

In the plot of the OPRs of NH_3 versus $^{14}\text{N}/^{15}\text{N}$ ratios in CN, we can find that comet 73P/SW3 is clearly separated from the main group (normal). This may indicate the existence of a second group as pointed out by Bonev et al. (2008a) based on the OPRs of water. Higher fractionation of ^{15}N corresponds to a higher OPR (i.e., lower T_{spin}) of NH_3 in the plot. Therefore, these facts also support the hypothesis that the OPR of NH_3 is a primordial character of cometary molecules. Although the D/H ratios of water had been obtained in only a small number of comets, their values clustered around 3×10^{-4} and the comets showing similar D/H ratios also show similar OPRs of NH_3 . This fact also supports the hypothesis that the OPR is one of the primordial properties of cometary ices. The peculiar nature of comet 73P/SW3 could be attributed to a different origin of icy materials in the solar nebula (e.g., difference in temperature, epoch, or chemical alterations).

The authors thank M. J. Mumma for his fruitful comments and suggestions as a referee. H. Kobayashi is a JSPS fellow of the Ministry of Education, Culture, Science and Technology (Japan). This work was financially supported by MEXT under Grant-in-Aid for Scientific Research 22540257 (H. Kawakita) and under Grant-in-Aid for “Private University Strategic Research Foundation Support Program.”

REFERENCES

A'Hearn, M. F., Millis, R. L., Schleicher, D. G., Osip, D. J., & Birch, P. V. 2005, *Icarus*, **118**, 223

Arpigny, C., Jehin, E., Manfroid, J., Hutsemékers, D., Schulz, R., Stüwe, J. A., Zucconi, J., & Ilyin, I. 2003, *Science*, **301**, 1522

Bird, M. K., Huchtmeier, W. K., Gensheimer, P., Wilson, T. L., Janardhan, P., & Lemme, C. 1997, *A&A*, **325**, L5

Biver, N., et al. 1999, *Earth Moon Planets*, **78**, 5

Biver, N., et al. 2006, *A&A*, **449**, 1255

Biver, N., et al. 2008, Asteroids, Comets, Meteors, Baltimore, Maryland, 2008 July 14–18, LPI Contribution No. 1405, 8149

Bockelée-Morvan, D., Woodward, C. E., Kelley, M. S., & Wooden, D. H. 2009, *ApJ*, **696**, 1075

Bockelée-Morvan, D., et al. 2000, *A&A*, **353**, 1101

Bockelée-Morvan, D., et al. 2001, *Science*, **292**, 1339

Böhnhardt, H., Mumma, M. J., Villanueva, G. L., DiSanti, M. A., Bonev, B. P., Lippi, M., & Käufl, H. U. 2008, *ApJ*, **683**, L71

Bonev, B. P., Mumma, M. J., Gibb, E. L., DiSanti, M. A., Villanueva, G. L., Magee-Sauer, K., & Ellis, R. S. 2009, *ApJ*, **699**, 1563

Bonev, B. P., Mumma, M. J., Kawakita, H., Kobayashi, H., & Villanueva, G. L. 2008a, *Icarus*, **196**, 241

Bonev, B. P., Mumma, M. J., Radeva, Y. L., DiSanti, M. A., Gibb, E. L., & Villanueva, G. L. 2008b, *ApJ*, **680**, L61

Bonev, B. P., Mumma, M. J., Villanueva, G. L., DiSanti, M. A., Ellis, R. S., Magee-Sauer, K., & Dello Russo, N. 2007, *ApJ*, **661**, L97

Boss, A. P. 2001, *ApJ*, **563**, 367

Cacciani, P., Cosléou, J., Khelkhal, M., Tudorie, M., Pizzaromo, C., & Pracna, P. 2009, *Phys. Rev.*, **80**, 42507

Capria, M. T., Cremonese, G., Boattini, A., de Sanctis, M. C., D'Abramo, G., & Buzzoni, A. 2002, in Asteroids, Comets, Meteors, ed. B. Warmbein (ESA-SP 500; Noordwijk, Netherlands: ESA), 693

Charnley, S. B., & Rodgers, S. D. 2008, *Space Sci. Rev.*, **138**, 59

Clough, S. A., & Iacono, M. J. 1995, *J. Geophys. Res.*, **100**, 159

Combi, M. R., Mäkinen, J. T. T., Bertaux, J.-L., Lee, Y., & Quémérais, E. 2009, *AJ*, **137**, 4734

Crovisier, J. 2006, *Faraday Discuss.*, **133**, 375

Crovisier, J. 2007, arXiv:astro-ph/0703785

Crovisier, J., Leech, K., Bockelée-Morvan, D., Brooke, T. Y., Hanner, M. S., Altieri, B., Keller, H. U., & Lellouch, E. 1997, *Science*, **275**, 1904

Dekker, H., D'Odorico, S., Kaufer, A., Delabre, B., & Kotzlowski, H. 2000, *Proc. SPIE*, **4008**, 534

Dello Russo, N., Bonev, B. P., DiSanti, M. A., Mumma, M. J., Gibb, E. L., Magee-Sauer, K., Barber, R. J., & Tennyson, J. 2005, *ApJ*, **621**, 537

Dello Russo, N., Mumma, M. J., DiSanti, M. A., Magee-Sauer, K., Gibb, E. L., Bonev, B. P., McLean, I. S., & Xu, L.-H. 2006, *Icarus*, **184**, 255

Dello Russo, N., Mumma, M. J., DiSanti, M. A., Magee-Sauer, K., & Novak, R. 2001, *Icarus*, **153**, 162

Dello Russo, N., Vervack, R. J., Weaver, H. A., Biver, N., Bockelée-Morvan, D., Crovisier, J., & Lisse, C. M. 2007, *Nature*, **448**, 172

DiSanti, M. A., Dello Russo, N., Magee-Sauer, K., Gibb, E. L., Reuter, D. C., & Mumma, M. J. 2001, Asteroids, Comets, Meteors (ESA SP-500, ESTEC; Noordwijk: ESA), 571

DiSanti, M. A., Villanueva, G. L., Bonev, B. P., Magee-Sauer, K., Lyke, J. E., & Mumma, M. J. 2007, *Icarus*, **187**, 240

Feldman, P. D., Cochran, A. L., & Combi, M. R. 2004, in Comet II, ed. M. C. Festou, H. U. Keller, & H. A. Weaver (Tucson, AZ: Univ. Arizona Press), 425

Fink, U. 2009, *Icarus*, **201**, 311

Gibb, E. L., DiSanti, M. A., Magee-Sauer, K., Dello Russo, N., Bonev, B. P., & Mumma, M. J. 2007, *Icarus*, **188**, 224

Gratton, R. G., et al. 2001, *Exp. Astron.*, **23**, 107

Grimm, R. E., & McSween, H. Y. 1993, *Science*, **259**, 653

Hersant, F., Gautier, D., & Hure, J.-M. 2001, *ApJ*, **554**, 391

Hily-Blant, P., Walmsley, M., Pineau des Forêts, G., & Flower, D. 2010, *A&A*, **513**, 41

Hutsemékers, D., Manfroid, J., Jehin, E., & Arpigny, C. 2009, *Icarus*, **204**, 346

Hutsemékers, D., Manfroid, J., Jehin, E., Arpigny, C., Cochran, A., Schulz, R., Stüwe, J. A., & Zucconi, J.-M. 2005, *A&A*, **440**, L21

Hutsemékers, D., Manfroid, J., Jehin, E., Zucconi, J.-M., & Arpigny, C. 2008, *A&A*, **490**, 31

Irvine, W. M., Schloerb, F. P., Crovisier, J., Fegley, B., Jr., & Mumma, M. J. 2000, in *Protostars and Planets IV*, ed. V. Mannings, A. P. Boss, & S. S. Russell (Tucson, AZ: Univ. Arizona Press), 1159

Jang-Condell, H. 2008, *ApJ*, **679**, 797

Jehin, E., Manfroid, J., Hutsemékers, D., Arpigny, C., & Zucconi, J.-M. 2009a, *Earth Moon Planets*, **105**, 167

Jehin, E., et al. 2002, *Earth Moon Planets*, **90**, 147

Jehin, E., et al. 2004, *ApJ*, **613**, L161

Jehin, E., et al. 2006, *ApJ*, **641**, L145

Jehin, E., et al. 2008, *LPICo*, **1405**, 8319

Jehin, E., et al. 2009b, *Earth Moon Planets*, **105**, 343

Jensen, P., Kraemer, W. P., & Bunker, P. R. 2003, *Mol. Phys.*, **101**, 613

Kawakita, H., Ayani, K., & Kawabata, T. 2000, *PASJ*, **52**, 925

Kawakita, H., Jehin, E., Manfroid, J., & Hutsemékers, D. 2007, *Icarus*, **187**, 272

Kawakita, H., & Kobayashi, H. 2009, *ApJ*, **693**, 388

Kawakita, H., & Watanabe, J. 1998, *ApJ*, **495**, 946

Kawakita, H., Watanabe, J., Furusho, R., Fuse, T., Capria, M. T., De Sanctis, M. C., & Cremonese, G. 2004, *ApJ*, **601**, 1152

Kawakita, H., Watanabe, J., Furusho, R., Fuse, T., & Boice, D. C. 2005, *ApJ*, **623**, L49

Kawakita, H., Watanabe, J., Fuse, T., Furusho, R., & Abe, S. 2002, *EM&P*, **90**, 371

Kawakita, H., Watanabe, J., Kinoshita, D., Ishiguro, M., & Nakamura, R. 2003, *ApJ*, **590**, 573

Kawakita, H., et al. 2001, *Science*, **294**, 1089

Kawakita, H., et al. 2006, *ApJ*, **643**, 1337

Kobayashi, H., Kawakita, H., Mumma, M. J., Bonev, B. P., Watanabe, J., & Fuse, T. 2007, *ApJ*, **668**, 75

Kobayashi, H., et al. 2010, *A&A*, **509**, 80

Kurucz, R. L. 2005, *Mem. Soc. Astron. Ital. Suppl.*, **8**, 189

Limbach, H., Buntkowsky, G., Matthes, J., Gründemann, S., Pery, T., Walaszek, B., & Chaudret, B. 2006, *Chem. Phys. Chem.*, **7**, 551

Lunine, J. I., Engel, S., Rizk, B., & Horanyi, M. 1991, *Icarus*, **94**, 333

Magee-Sauer, K., Mumma, M. J., DiSanti, M. A., & Dello Russo, N. 2001, American Astronomical Society, 33rd DPS Meeting, 20.09

Magee-Sauer, K., Mumma, M. J., DiSanti, M. A., & Dello Russo, N. 2002, *J. Geophys. Res.*, **107**, 5096

Magee-Sauer, K., Mumma, M. J., DiSanti, M. A., Dello Russo, N., Gibb, E. L., Bonev, B. P., & Villanueva, G. L. 2008, *Icarus*, **194**, 347

Manfroid, J., Jehin, E., Hutsemékers, D., Cochran, A., Zucconi, J.-M., Arpigny, C., Schulz, R., & Stüwe, J. A. 2005, *A&A*, **432**, 5

Manfroid, J., et al. 2009, *A&A*, **503**, 613

Meech, K. J., & Svoren, J. 2004, in *Comet II*, ed. M. C. Festou, H. U. Keller, & H. A. Weaver (Tucson, AZ: Univ. Arizona Press), 317

Meier, R., Owen, T. C., Matthews, H. E., Jewitt, D. C., Bockelée-Morvan, D., Biver, N., Crovisier, J., & Gautier, D. 1998, *Science*, **279**, 842

Messenger, S., Stadermann, F. J., Floss, C., Nittler, L. R., & Mukhopadhyay, S. 2003, *Space Sci. Rev.*, **106**, 155

Morbidelli, A. 2008, in *Trans-Neptunian Objects and Comets*, (Saas-Fee Advanced Course 35; Swiss Society for Astrophysics and Astronomy), ed. D. Jewitt, A. Morbidelli, & H. Rauer (Berlin: Springer), 79

Mumma, M. J., DiSanti, M. A., Dello Russo, N., Magee-Sauer, K., Gibb, E., & Novak, R. 2003, *Adv. Space Res.*, **31**, 2563

Mumma, M. J., Weaver, H. A., & Larson, H. P. 1987, *A&A*, **187**, 419

Mumma, M. J., Weissman, P. R., & Stern, S. A. 1993, *Protostars and Planets III* (Tucson, AZ: Univ. Arizona Press), 1177

Mumma, M. J., et al. 2001, *Science*, **292**, 1334

Mumma, M. J., et al. 2005, *Science*, **310**, 270

Noguchi, T., Ando, H., Izumiura, H., Kawanomoto, S., Tanaka, W., & Aoki, W. 1998, *Proc. SPIE*, **3355**, 354

Onishi, R., Shinnaka, Y., Kobayashi, H., & Kawakita, H. 2008, American Astronomical Society, 40th DPS Meeting, 16.09

Pardanaud, C., Crovisier, J., Bockelée-Morvan, D., & Biver, N. 2007, *Molecules in Space and Laboratory*, ed. J. L. Lemaire & F. Combes (Paris: Obs. Paris)

Podolak, M., & Prialnik, D. 1996, *Planet. Space Sci.*, **44**, 655

Prialnik, D., Festiy, M. C., Keller, H. U., & Weaver, H. A. 2004, *Comets II* (Tucson, AZ: Univ. Arizona Press), 359

Quack, M. 1977, *Mol. Phys.*, **34**, 477

Radeva, Y. L., Mumma, M. J., Bonev, B. P., DiSanti, M. A., Villanueva, G. L., Magee-Sauer, K., Gibb, E. L., & Weaver, H. A. 2010, *Icarus*, **206**, 764

Rodgers, S. D., & Charnley, S. B. 2008a, *ApJ*, **689**, 1448

Rodgers, S. D., & Charnley, S. B. 2008b, *MNRAS*, **385**, 48

Rosenberg, E. D., & Prialnik, D. 2007, *New Astron.*, **12**, 523

Schleicher, D. G., & Bair, A. N. 2008, *Asteroids, Comets, Meteors*, Baltimore, Maryland, 2008 July 14–18, LPI Contribution No. 1405, 8174

Shinnaka, Y., Kawakita, H., Kobayashi, H., & Kanda, Y. 2010, *PASJ*, **62**, 263

Uy, D., Cordinnier, M., & Oka, T. 1997, *Phys. Rev. Lett.*, **78**, 3844

Villanueva, G. L., Bonev, B. P., Mumma, M. J., Magee-Sauer, K., DiSanti, M. A., Salyk, C., & Blake, G. A. 2006, *ApJ*, **650**, 87

Villanueva, G. L., Mumma, M. J., Bonev, B. P., DiSanti, M. A., Gibb, E. L., Boehnhardt, H., & Lippi, M. 2008, *Asteroids, Comets, Meteors*, LPI Contribution No. 1405, 8393

Villanueva, G. L., Mumma, M. J., Bonev, B. P., DiSanti, M. A., Gibb, E. L., Boehnhardt, H., & Lippi, M. 2009, *ApJ*, **690**, L5

Weaver, H. A., A'Hearn, M. F., Arpigny, C., Combi, M. R., Feldman, P. D., Tozzi, G.-P., Dello Russo, N., & Festou, M. C. 2008, *Asteroids, Comets, Meteors*, LPI Contribution No. 1405, 8216

Weaver, H. A., et al. 2001, *Science*, **292**, 1329

Willacy, K., Klahr, H. H., Millar, T. J., & Henning, Th. 1998, *A&A*, **338**, 995

Woodward, C. E., Kelley, M. S., Bockelée-Morvan, D., & Gehr, R. D. 2007, *ApJ*, **671**, 1065

Zhao, G., & Li, H.-B. 2001, *Chin. J. Astron. Astrophys.*, **1**, 555